

DOE/MC/28055-95/C0496<sup>✓</sup>

**Tubular Solid Oxide Fuel Cell Developments**

**Authors:**

R.J. Bratton  
P. Singh

Conf-9505249--9

**Contractor:**

Westinghouse Electric Corporation  
Science and Technology Center  
1310 Beulah Road  
Pittsburgh, Pennsylvania 15235

**Contract Number:**

DE-FC21-91MC28055

**Conference Title:**

97th Annual Meeting of the American Ceramic Society

**Conference Location:**

Cincinnati, Ohio

**Conference Dates:**

May 1-3, 1995

**Conference Sponsor:**

DOE

## **DISCLAIMER**

**Portions of this document may be illegible in electronic image products. Images are produced from the best available original document.**

## A REVIEW OF TUBULAR SOLID OXIDE FUEL CELL DEVELOPMENTS

R. J. Bratton and P. Singh  
Westinghouse Electric Corporation  
Science & Technology Center  
Pittsburgh, PA 15235

### ABSTRACT

An overview of the tubular solid oxide fuel cell (SOFC) development at Westinghouse is presented in this paper. The basic operating principles of SOFCs, evolution in tubular cell design and performance improvement, selection criteria for cell component materials, and cell processing techniques are discussed. The commercial goal is to develop a cell that can operate for 5 to 10 years. Results of cell test operated for more than 50,000 hours are presented. Since 1986, significant progress has been made in the evolution of cells with higher power, lower cost and improved thermal cyclic capability. Also in this period, successively larger multi-kilowatt electrical generators systems have been built and successfully operated for more than 7000 hours.

### INTRODUCTION

Solid oxide fuel cell (SOFC) power generation systems are capable of producing electricity at higher electrical efficiency with minimal environmental impact than any competing technology. Simple cycle efficiency of 50% (net AC/HHV  $\text{CH}_4$ ) and combined cycle electrical efficiency of >55% are readily achievable in commercial units. In addition, Nitrous oxide ( $\text{NO}_x$ ) emissions in the exhaust product streams have been repeatedly measured at 0.3 ppm which is an order of magnitude below that measured for competing non-fuel cell technologies. SOFC power generation systems operating at 1000°C provide high quality byproduct heat and can operate directly on unprocessed natural gas via internal reforming thus eliminating the need for an external reforming system for fuel processing. Fuel cell systems also offer advantages of the modularity of construction, low noise operation and multiplicity of fuel use.

The most progress to date has been made with tubular cell designs that employ a dense yttria stabilized zirconia thin film as the electrolyte, doped

lanthanum manganite as the air electrode, nickel-zirconia cermet as the fuel electrode, and doped lanthanum chromite as the cell interconnection. Selection of these materials is based on their closely matched thermal expansion coefficients, high temperature electrical properties and long term chemical and structural stabilities. Single cell operation for more than 50,000 hours and generator operation for more than 7000 hours have been successfully demonstrated. This paper discusses tubular SOFC developments at Westinghouse in terms of cell technology and multi-kilowatt generator system demonstration activities.

## SOFC TECHNOLOGY BACKGROUND

High temperature solid oxide fuel cells are direct energy conversion electrochemical devices where chemical energy derived from the electrochemical oxidation of the fuel is continuously converted into electrical energy. In the most basic form, solid oxide fuel cells consist of an anode (exposed to the fuel) and a cathode (exposed to the oxidant) electrode separated by a dense predominantly oxygen ion conducting electrolyte layer. The two porous electrodes are connected by a resistive load. The electro-chemical oxidation of the fuel at the anode electrode produces electrons which flow through the external circuit to the cathode electrode on which oxygen is reduced. A schematic representation of the electrochemical processes and the various cell reactions are shown in Figure 1.

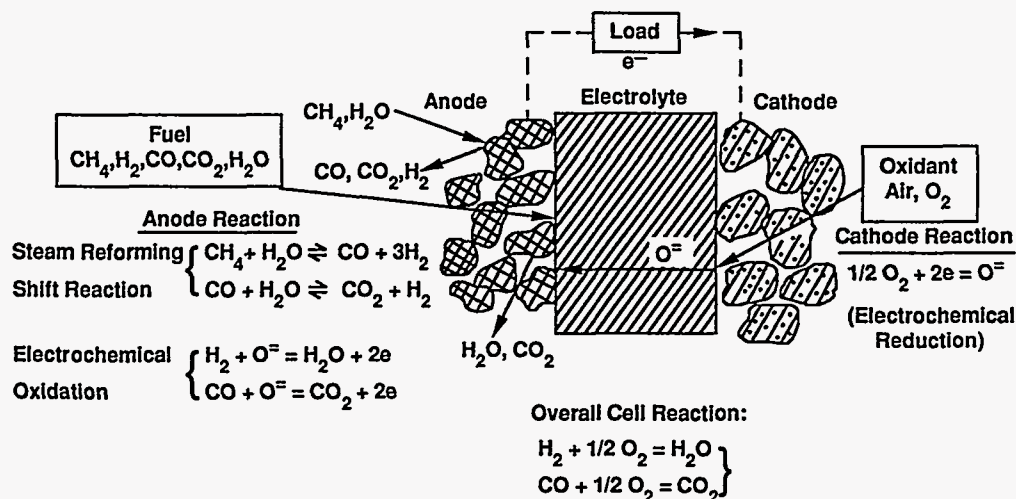


Figure 1 – Schematic presentation of electrochemical processes and overall cell reactions in solid oxide fuel cells.

The Nernst voltage  $E_{\text{Nernst}}$  of the electrochemical cell is given by

$$E_{\text{Nernst}} = t_i \cdot R \cdot T / n \cdot F \ln ( P_{\text{O}_2}'' / P_{\text{O}_2}' ) \quad [1]$$

where  $P_{\text{O}_2}''$  and  $P_{\text{O}_2}'$  are oxygen partial pressures (in atm.) in the fuel and the oxidant gas atmospheres,  $t_i$  is the ionic transport number of the electrolyte material,  $n$  is the number of electrons participating in the ionic transport and  $RT$  and  $F$  have their usual meanings. Cell terminal voltage  $E_{\text{terminal}}$  (volts) which is lower than the Nernst voltage due to the resistive and electrode polarization losses, is given by

$$E_{\text{terminal}} = E_{\text{Nernst}} - i \cdot \Omega - \eta \quad [2]$$

where  $i$  is the current density (amp/cm<sup>2</sup>),  $\Omega$  is the internal cell resistance (ohm.cm<sup>2</sup>) and  $\eta$  is the overall electrode polarization loss (diffusional and activation polarization losses in volts). From Eqs. [1] and [2], it is evident that to achieve the highest possible cell terminal voltage at a given cell temperature and in a given fuel and oxidant composition, both cell internal resistance and electrode polarizations need to be minimized.

Operation of the solid oxide fuel cell containing an oxygen ion conducting yttria-stabilized zirconia electrolyte was first demonstrated by Baur and Pries in 1937<sup>(1)</sup>. The work of Weissbart and Ruka<sup>(2)</sup> demonstrated the operation of a solid oxide fuel cell (calcia-stabilized zirconia electrolyte and porous platinum electrodes) on both hydrogen and hydrocarbon fuels. The feasibility of a "multi" cell 100 kWe solid oxide fuel cell generator of a bell and spigot design fabricated using thin film (0.03-0.04 mm thick electrolyte layer produced by reactive sintering) calcia-stabilized zirconia electrolyte, noble metal electrodes, and Lanthanum chromite cell to cell interconnect was demonstrated by Archer et.al.<sup>(3)</sup> in 1965.

Use of a lower cost nickel-zirconia cermet fuel electrode and electronically conducting oxide air electrodes as substitutes for noble metal electrodes was subsequently demonstrated by Arcossi and Bergman<sup>(4)</sup> and Spacil and Tedman<sup>(5)</sup>. The basis for selection of the conducting oxide air electrodes, and the materials limitations related to the chemical compatibility with adjoining components, thermal expansion mismatch etc., were also discussed by the authors. In 1972, Fisher et.al.<sup>(6)</sup> described the fabrication and performance of thin wall cylindrical fuel cells which incorporated an yttria-stabilized zirconia electrolyte, a conducting oxide air electrode, and a nickel-zirconia fuel electrode. The fuel cells described above showed limited electrical performance due to higher cell internal resistance. Additionally, these cells were

found to have a limited operating life and poor performance stability due to premature cell component failure and interfacial reaction products formation.

Isenberg<sup>(7)</sup> developed thin film tubular solid oxide fuel cells and operated a three cell stack of this design using a  $H_2$ - $H_2O$  gas mixture as the fuel and air as the oxidant. Cells were operated at  $1000^\circ C$  for more than 8700 hours<sup>(8)</sup>. In the tubular fuel cell design, thin electrochemically active cell component layers were deposited on a closed end porous calcia-stabilized zirconia support tube. The active cell component layers consisted of a porous, doped lanthanum manganite air electrode layer (1.0-1.4 mm thick), a dense yttria-stabilized zirconia electrolyte layer (30-40  $\mu M$  thick), a dense, doped lanthanum chromite interconnection layer (30-40  $\mu M$  thick), and a porous nickel-zirconia cermet fuel electrode (100-120  $\mu M$  thick). A schematic of the cell cross section is shown in Figure 2.

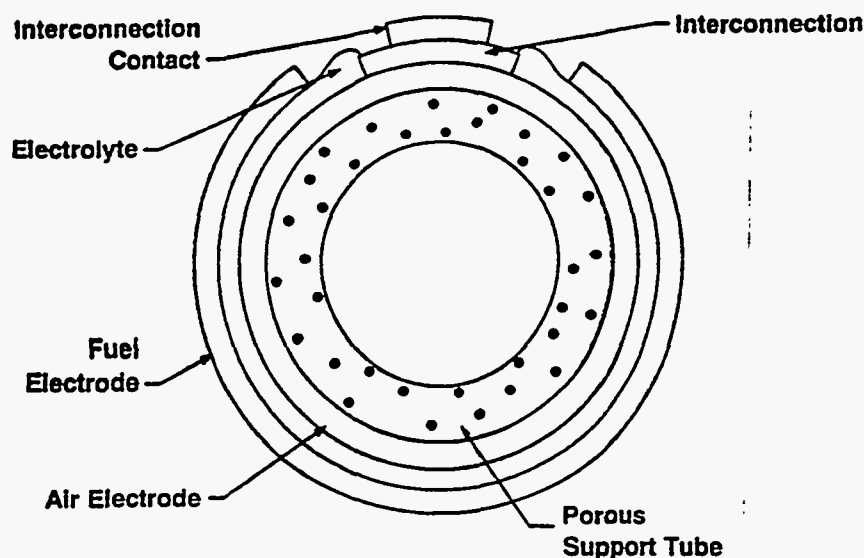


Figure 2 – Cross section of a tubular design solid oxide fuel cell

#### CELL COMPONENT MATERIALS SELECTION BASIS

Stable long term operation of solid oxide fuel cells requires that the individual cell components remain chemically and structurally stable during prolonged periods at elevated temperatures. Cell component materials selection has essentially been dictated by functional requirements, and chemical and structural stabilities.

## Functional Requirements

Successful solid oxide fuel cell operation requires that the electrical and electrochemical functional characteristics of cell component materials are preserved during long term high temperature operation. The candidate electrolyte material must remain predominantly an ionic conductor (within the electrolytic domain) in the fuel and the oxidant gas streams to prevent the formation of internal electronic shorting which is parasitic to the cell. The electrolyte layer must also provide an impervious gaseous permeation barrier layer between the fuel and the oxidant to prevent the direct combustion of the fuel due to the intermixing of fuel and oxidants. Similarly, the cell interconnect layer must provide a gaseous permeation barrier, and the interconnect material should demonstrate predominantly electronic conduction behavior in both fuel and oxidant atmospheres. Lack of ionic conduction in the interconnection material minimizes the ionic transport of the oxidant and hence prevents localized fuel combustion. For fuel cell electrodes, electrocatalytic activity for the oxidation of the fuel and the reduction of the oxidants must be maintained in the cell electrode materials over the entire life time of the cell. Electrode materials must demonstrate small over potentials for electrochemical reactions and favor faster electrode kinetics to support high current density operation of the fuel cells. Finally, the electrode materials and the electrocatalytic sites must remain resistant to poisoning caused either by interface or gas phase assisted contamination.

## Chemical Requirements

Materials selected for cell component fabrication should show bulk as well as interfacial stability (compositional and phase stability) during cell fabrication processes and long term electrical operation. The selected electrolyte material should preserve its lattice defect structure (lattice with oxygen ion vacancy) in both fuel and oxidant gas atmospheres and also remain stable in contact with adjacent electrodes to prevent the formation of interfacial reaction products. Reaction products formed at the electrode-electrolyte interfaces can lead to an increase in the cell resistance and reduction in the electrocatalytic activity of the electrodes (electrode kinetics). Selection of cell interconnection material is similarly based on the bulk stability of the material in the fuel and the oxidant gases and the interfacial stability with the air electrode. The compositional and structural (crystal/lattice) stability of the cell electrode materials are very important for maintaining cell electrical performance over long operating periods.



## Structural Requirements

Cell component materials and their well defined structures must remain dimensionally stable during the cell fabrication processes and electrical operation to prevent the development of damaging stresses in the various cell components. Thermal expansion coefficients of the cell component materials should be matched over the cell fabrication and operating temperature range to prevent the cracking or separation of the cell components when exposed to isothermal or thermal cyclic conditions. Sintering-resistant fuel cell electrode structures are also desired for minimizing interfacial stress buildup. Sintering-resistant electrodes also help to maintain the porous electrode structure which provides gas diffusion paths to the reacting interfaces. In the case of tubular designs, the support tube must maintain structural integrity during cell fabrication and operation.

In addition to the above requirements, cell component materials must also remain cost effective, commercially available and easy to fabricate.

## CELL COMPONENT MATERIALS AND FABRICATION PROCESSES

Minh<sup>(9)</sup> has presented a review of SOFC component materials and fabrication processes currently being used for fabricating ceramic fuel cells. Evolution of cell component technology (Table 1) for tubular solid oxide fuel cell has been reviewed by Kinoshita et.al.<sup>(10)</sup>. This paper summarizes the advanced tubular cell component materials and fabrication processes. The Westinghouse advanced tubular fuel cell design consists of an air electrode supported configuration wherein a porous air electrode tube (closed at one end) serves the dual function of the air electrode and the support structure for the dense electrolyte, interconnection and the fuel electrode layers. Cell component materials and fabrication processes are presented below.

### Electrolyte

Among various zirconia based and other oxygen ion conducting electrolyte materials currently being developed and evaluated for SOFC applications<sup>(11,12,13)</sup>, yttria stabilized zirconia (YSZ) serves as the electrolyte material of choice for tubular cell fabrication because of its higher electrical conductivity<sup>(14)</sup>, desirable electrolytic domain<sup>(15)</sup>, long term chemical and structural stability and the ease of fabrication. The incorporation of yttria in the host zirconia lattice creates oxygen ion vacancies by charge compensation according to Eq. [3].





Table 1  
Evolution of Tubular Solid Oxide Fuel Cell Component  
Material and Fabrication Technology<sup>(10)</sup>

Component	ca. 1965	ca. 1975	Current Status <sup>a</sup>
Anode	<ul style="list-style-type: none"> <li>• porous Pt</li> </ul>	<ul style="list-style-type: none"> <li>• Ni-ZrO<sub>2</sub> cermet<sup>b</sup></li> </ul>	<ul style="list-style-type: none"> <li>• Ni-ZrO<sub>2</sub> cermet<sup>b</sup></li> <li>• deposit slurry</li> <li>• -150-<math>\mu</math>m thickness</li> <li>• 20-40% porosity</li> </ul>
Cathode	<ul style="list-style-type: none"> <li>• porous Pt</li> </ul>	<ul style="list-style-type: none"> <li>• stabilized ZrO<sub>2</sub> impregnated with praesodymium oxide</li> </ul>	<ul style="list-style-type: none"> <li>• Sr-doped lanthanum manganite</li> <li>• deposit slurry, sinter</li> <li>• -1-mm thickness</li> <li>• 20-40% porosity</li> </ul>
Electrolyte	<ul style="list-style-type: none"> <li>• yttria-stabilized ZrO<sub>2</sub></li> <li>• 0.5-mm thickness</li> </ul>	<ul style="list-style-type: none"> <li>• yttria-stabilized ZrO<sub>2</sub></li> <li>• EVD</li> </ul>	<ul style="list-style-type: none"> <li>• yttria-stabilized ZrO<sub>2</sub></li> <li>• EVD</li> <li>• -40-<math>\mu</math>m thickness</li> </ul>
Cell Inter-connect	<ul style="list-style-type: none"> <li>• Pt</li> </ul>	<ul style="list-style-type: none"> <li>• Mn-doped cobalt chromite</li> </ul>	<ul style="list-style-type: none"> <li>• Mg-doped lanthanum chromite</li> <li>• EVD</li> <li>• -40-<math>\mu</math>m thickness</li> </ul>
Support Tube	<ul style="list-style-type: none"> <li>• yttria-stabilized ZrO<sub>2</sub></li> </ul>	<ul style="list-style-type: none"> <li>• yttria-stabilized ZrO<sub>2</sub></li> </ul>	<ul style="list-style-type: none"> <li>• calcia-stabilized ZrO<sub>2</sub></li> <li>• 34-35% porosity</li> <li>• 12.8-mm diameter</li> <li>• 1-2-mm wall thickness</li> <li>• 457-mm length</li> </ul>

<sup>a</sup> Specifications for Westinghouse 5-kW fuel cell

<sup>b</sup> Y<sub>2</sub>O<sub>3</sub>-stabilized ZrO<sub>2</sub>

EVD = electrochemical vapor deposition

where  $(Y)'_{Zr}$  indicates Y ion on Zr lattice site,  $(V''_O)$  is the oxygen ion vacancy and  $(O^x)$  is the neutral oxygen on the oxygen lattice site. The defects in the lattice have been considered randomly distributed.

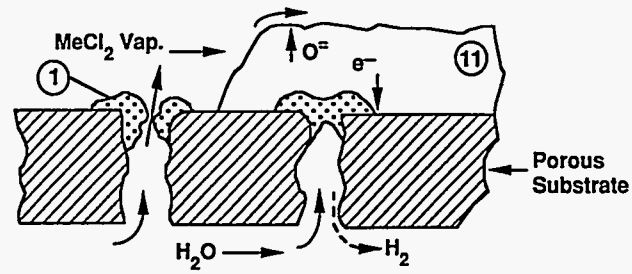
With sufficient  $Y_2O_3$  dopant substitution (>6 mol %) in the host lattice, the cubic fluorite structure of the zirconia remains stabilized over a wide temperature range (room temperature to cell fabrication temperatures) and eliminates transformations to monoclinic or tetragonal modifications of pure zirconia. The oxygen ion conduction in the stabilized zirconia results from the movement of oxygen ions through vacancies and increased conductivity results from improved oxygen ion mobility in the lattice. The ionic transport number of the electrolyte material remains close to unity (electrolytic domain) in a wide oxygen partial pressure range (typical fuel and oxidant atmospheres of the fuel cells). Predominantly ionic behavior and the absence of electronic conduction in the electrolyte layer prevents internal parasitic cell formation and loss of power during cell operation. Maximum conductivity in the zirconia has been observed at 8-10 mol %  $Y_2O_3$  dopant concentration levels beyond which the conductivity decreases sharply because of defect ordering<sup>(16)</sup>.

A thin dense YSZ electrolyte layer for the tubular SOFC application has generally been fabricated by an Electrochemical Vapor Deposition (EVD) technique<sup>(17)</sup> as shown schematically in Figure 3. During the initial nucleation and substrate pore closure stage of the film growth, gas phase reactions between Zr,Y chlorides and  $H_2O, O_2$  remain responsible for the formation of the initial zirconia film. After pore closure, however, the film growth predominantly takes place due to the interaction of Zr,Y chlorides with the oxygen ions (diffusing through the electrolyte film). The electrolyte film grows with oriented columnar grains and is approximately 30 to 40  $\mu m$  thick after 40 minutes deposition time (reaction temperature  $\sim 1200^\circ C$ ). Figure 4 shows a polished and etched cross section of an electrolyte film grown by EVD.

X-ray diffraction and microprobe analysis have confirmed that these films have cubic structure and show a homogeneous distribution of yttrium in the bulk. The electrolyte films have remained leak tight during prolonged high temperature exposure. Segregation of dopants and contaminants have not been detected in these films.

### Cell Electrodes

Porous nickel-zirconia cermet and doped lanthanum manganite electrode materials have been successfully used as the anode (fuel) and the cathode (air) electrodes during the manufacture and operation of the advanced tubular



Phase I — Pore Closure by CVD  
 $\text{MeCl}_2 + \text{H}_2\text{O} \rightarrow \text{MeO} + 2 \text{HCl}$

Phase II — Scale Growth by EVD  
 $\text{MeCl}_2 + \text{O}^{2-} \rightarrow \text{MeO} + \text{Cl}_2 + 2\text{e}^-$   
 $\text{H}_2\text{O} + 2\text{e}^- \rightarrow \text{H}_2 + \text{O}^{2-}$

Figure 3 – A schematic of the EVD electrolyte film growth process.

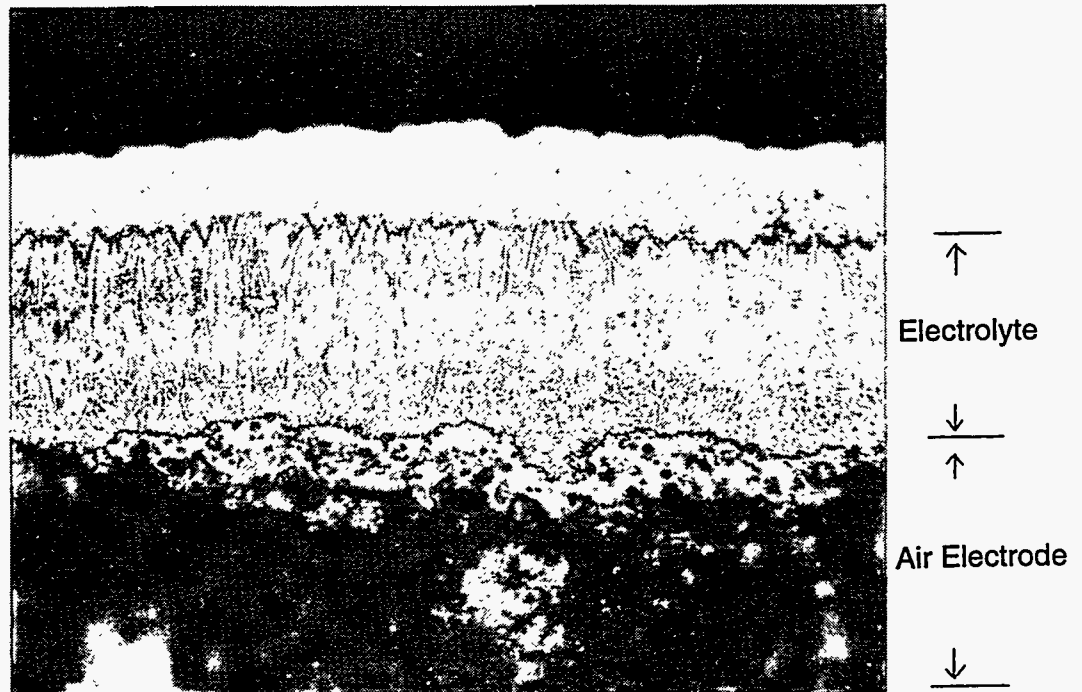


Figure 4 – EVD grown electrolyte film microstructure (magnification X500).

air electrode supported cells. The successful use of non noble materials for electrodes has significantly reduced the cell material cost and thereby enhanced the practicality of the fuel cell.

#### Anode Electrode

The nickel-zirconia cermet fuel electrode, in contact with the electrolyte layer and exposed to the fuel gas, is thermodynamically stable during cell operation (in fuel gas compositions representing more than 95% fuel utilizations) and shows very small to negligible activational and diffusional polarization losses (<15 mV) at 1000°C. The presence of the well distributed zirconia particles (yttria stabilized) in the cermet electrode inhibits sintering and coalescence of the nickel metal particles, thus improving the structural stability during the prolonged high temperature exposure. This type of cermet fuel electrode also maintains good physical contact with the electrolyte layer during isothermal and thermal cyclic exposure conditions due to the bonding developed because of a zirconia layer contact. The electrical conductivity of the cermet electrode material shows large dependence on the nickel content<sup>(18)</sup>. A significant increase in the conductivity of the electrode is observed around 30 vol % nickel due to nickel-nickel contacts establishing an electronic path which otherwise stays broken due to the presence of zirconia.

The nickel-zirconia cermet fuel electrode is fabricated by a combined slurry deposition- EVD process. Porous nickel powder slurry (~100-150 μm thick) is first applied over the electrolyte surface and subsequently fixed in situ with a thin zirconia layer using the EVD process. The mechanism for the zirconia layer formation over the nickel particle network is similar to the electrolyte growth process.

#### Cathode Electrode

Doped lanthanum manganites ( $\text{La}_x\text{M}_{1-x}\text{MnO}_3$  where M is Sr, Ca etc.) have commonly been used as the air electrode materials for the fabrication of tubular fuel cells because of their lower cost, high electrical conductivity at cell operating temperature (0.0075 to 0.01 ohm  $\text{cm}^{-1}$  at 1000°C), closely matched thermal expansion coefficient with the electrolyte, stability in the oxidizing atmosphere and low over voltage for the oxygen reduction. Electrical conductivity of several doped lanthanum manganites is shown in Figure 5. The electronic conduction takes place via a small polaron conduction mechanism. It is observed from the conductivity data that by increasing the dopant concentration, the electronic conductivity increases due to change in the Mn<sup>4+</sup> concentration in the lattice (Eq. [4]).

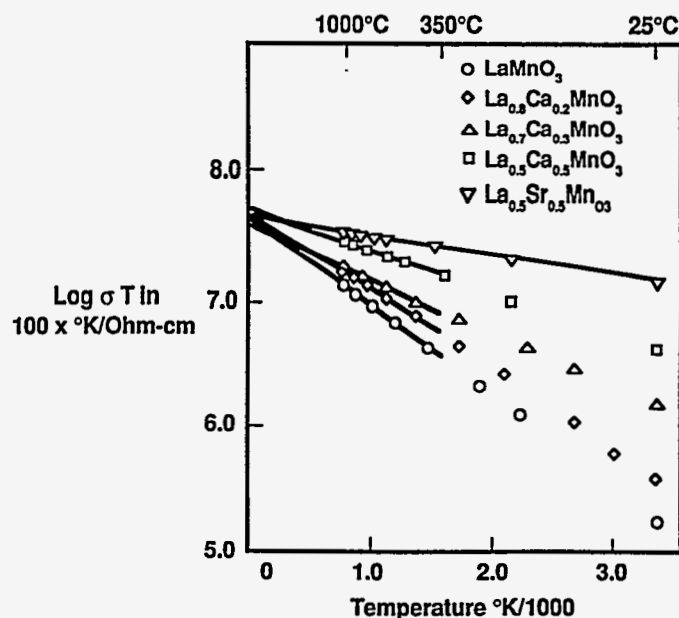
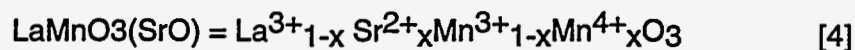


Figure 5 – Electrical conductivity of doped lanthanum manganite.



Doped lanthanum manganite is a p-type conductor and possesses a distorted perovskite (rhombohedral) lattice structure. Oxygen content depends on the temperature and the surrounding oxygen pressure and can vary from an oxygen deficiency to stoichiometry to an oxygen excess composition. The oxide lattice which shows an oxygen excess at higher oxygen pressure (metal ion vacancies) changes to an oxygen deficient (oxygen ion vacancies) lattice at lower oxygen pressures as shown in Figure 6. Anionic and cationic vacancies in air electrode materials have been proposed to greatly influence their electrical and electrochemical behavior<sup>(19)</sup>. The air electrode material has also been found to remain stable in contact with the electrolyte material<sup>(20,21)</sup> during cell operation and fabrication. Porous air electrode tubular structures have been fabricated by standard extrusion-sintering processes. Air electrode tubes of up to 2 m length have been successfully extruded and sintered for cell fabrication.

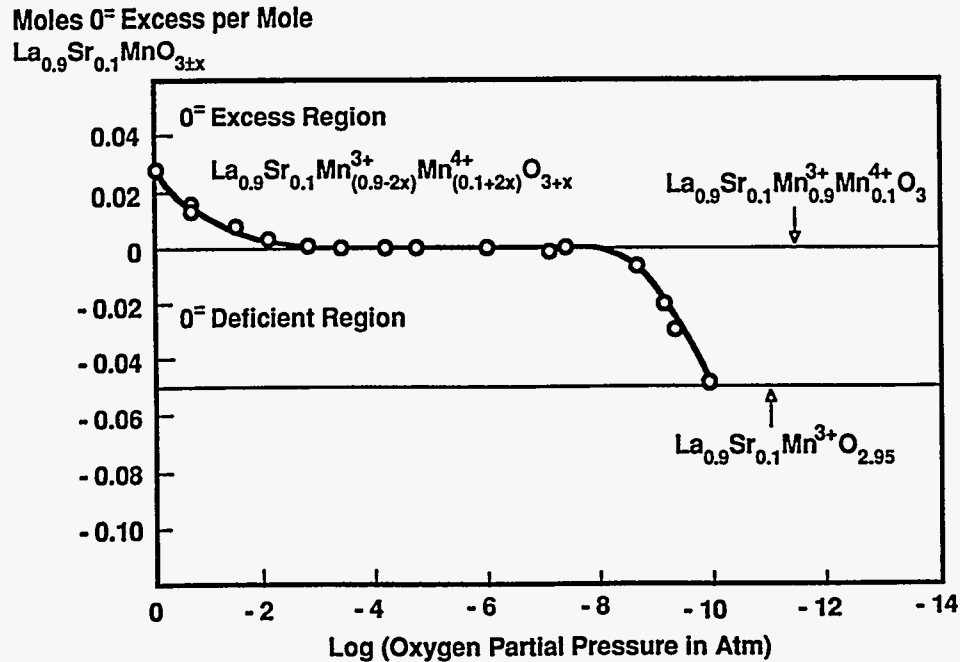


Figure 6 – Change in the oxygen stoichiometry of strontium doped lanthanum manganite at 1000°C.

#### CELL INTERCONNECTION

Cell to cell electrical connection, utilizing inexpensive electronic conductors which remain stable in a wide range of oxygen partial pressures (representative of the fuel and oxidant gas atmospheres), has been achieved through the use of electronic oxide conductors. Lanthanum chromites doped with alkaline earth cations and possessing perovskite structures, in particular, have been found very attractive because of their low reactivity with cell components, high electronic conductivity and composition invariance in fuel and oxidant gas atmospheres<sup>(22)</sup>. Electronic conduction in doped lanthanum chromites takes place by adiabatic hopping of positive holes as small polarons, and an increase in the conductivity is achieved by increasing the dopant level concentrations, which in turn increases the charge carrier concentration<sup>(23)</sup>. The electrical conductivity of several doped lanthanum chromites is shown in Figure 7. Dense magnesium-doped lanthanum chromite films (~40 to 50  $\mu$ m thick) have been grown over the porous air electrode support structures by the EVD technique.

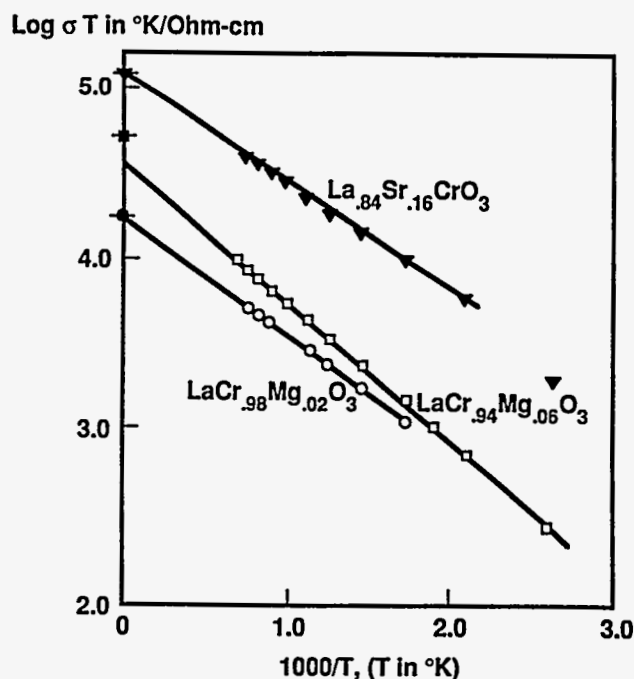


Figure 7 – Electrical conductivity of doped lanthanum chromites.

#### TUBULAR SOFC CELL DESIGN AND PERFORMANCE

Among the various solid oxide fuel cell configurations currently being developed world wide [planar<sup>(24)</sup>, segmented<sup>(25)</sup> and monolithic cell designs<sup>(26)</sup>], most progress to date has been made with the tubular cell geometry. A large number of PST (porous support tube) type cells have been electrically tested in  $H_2$ - $H_2O$  and hydrocarbon fuels<sup>(27,28)</sup> in the temperature range of 875 to 1200°C. These cells have shown excellent performance and long term performance stability. Single cell tests have been conducted for more than 50,000 hours with less than 0.5% per thousand hours voltage degradation, as shown in Figure 8. Several multi kilowatt generators employing such tubular cells have also been successfully field tested as discussed in a later section.

Several modifications of the tubular fuel cell designs have evolved in the pursuit of cell cost reduction and improved electrical performance. The early tubular fuel cells were fabricated using 2 mm thick porous support tubes (called thick wall PST). Although sufficiently porous to allow oxygen diffusion through to the air electrode, the thick PST increased the diffusional polarization of the



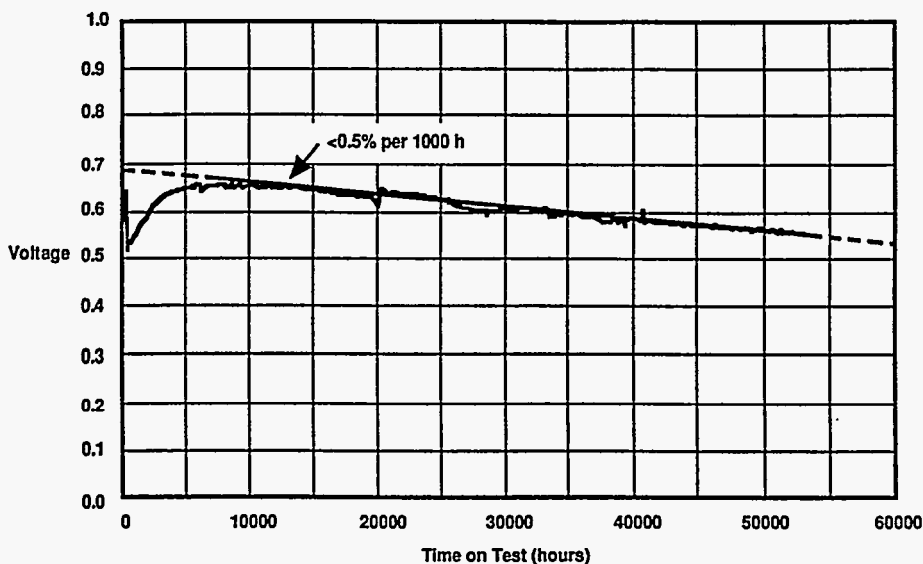


Figure 8 – Long term electrical performance of a PST type solid oxide fuel cell. Voltage degradation is below 0.5% per thousand hours.

cells resulting in significant performance losses. Therefore, the reduction of the PST wall thickness became the focus of subsequent experimentations. Initially, the PST wall thickness was reduced from 2 mm to 1.2 mm (the thin wall PST), which resulted in a significant reduction in the air electrode polarization. Ultimately, the porous support tube was completely eliminated from the fuel cell structure by the extruded air electrode tube (one end closed) of 1.9 mm thickness. In this configuration, the air electrode tube not only supported various cell components but also remained electrochemically active for oxygen reduction during cell operation. Elimination of the porous support tube from the cell structure resulted in a significant cell cost reduction and improvement in air electrode performance due to reduction in the polarization losses during cell operation. Fuel cell component materials and fabrication techniques (deposition of cell component layers) for air electrode supported structures remained similar to PST type cell fabrication. Figures 9 and 10 show the schematic configurations of the porous support and the air electrode supported tubular solid oxide fuel cell designs, respectively.

The air electrode supported (AES) tubular fuel cells have consistently shown better electrical performance than PST cells. Figure 11 shows the voltage output of a typical air electrode supported cell (50 cm active cell length, 1.56 cm diameter). The cell was operated at 1000°C cell average temperature, 450 mA/cm<sup>2</sup> current density, 85% fuel (H<sub>2</sub>-11% H<sub>2</sub>O) and 25% oxidant (air) utilizations. A comparison of the current-voltage characteristics for various cell designs are shown in Figure 12.

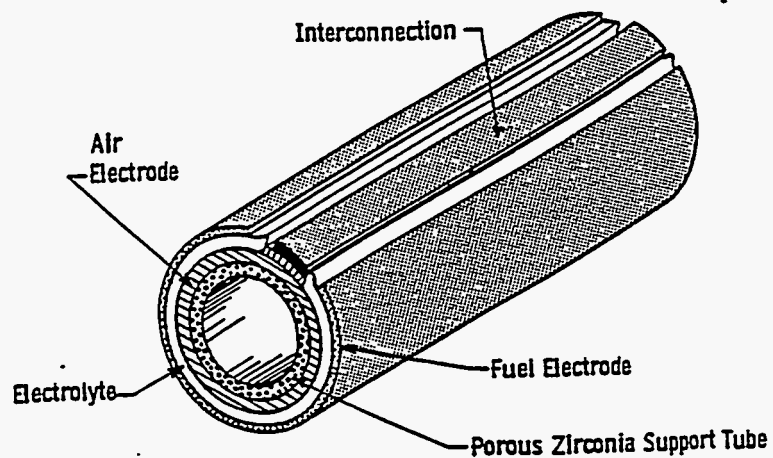


Figure 9 – Porous support tube (PST) type tubular fuel cell.

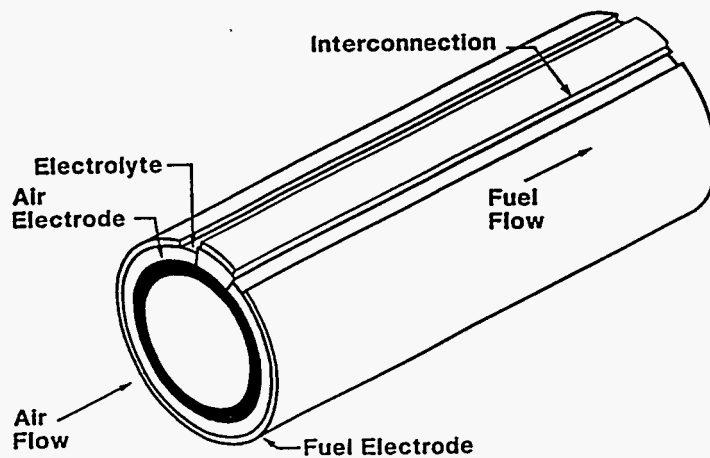


Figure 10 – Air electrode supported tubular solid oxide fuel cell design.

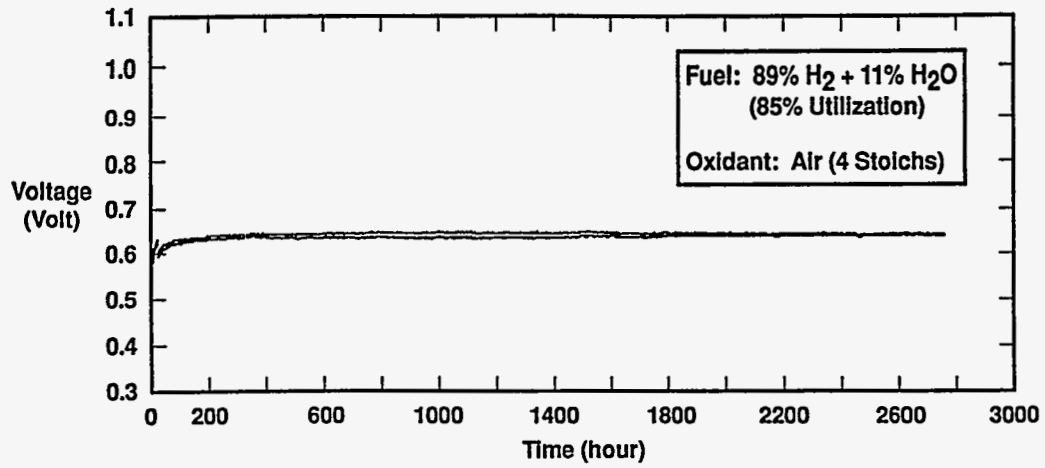


Figure 11 – Electrical performance behavior of a typical air electrode supported cell at 1000°C and 450 mA/cm<sup>2</sup>.

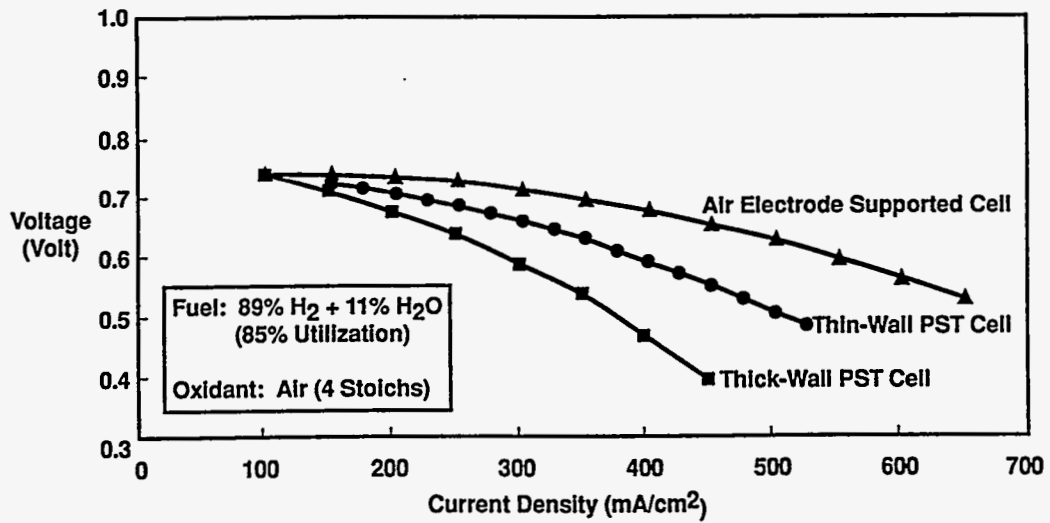


Figure 12 – Comparison of the voltage-current behavior of tubular fuel cell designs at 1000°C.

Apart from eliminating the support tube structure from the cell design, cell development efforts have also been focused on increasing the active electrochemical area of the cell through increases in the active length and diameter of the tubular fuel cells. The combined effects of increasing the cell length from 30 cm to 100 cm and eliminating the PST has resulted in a six fold increase in the cell power output (Figure 13). Longer cells of 1.5 to 2 m long are currently being evaluated in an attempt to further increase the cell power output. A larger cell power output reduces the number of cells required for a given size power generator thus reducing the overall cost of the power generation system.

#### TUBULAR SOFC GENERATOR DESIGN & DEMONSTRATION ACTIVITIES

During the tubular cell operation (Figure 14), air is introduced to the inside of the fuel cell through an air injector tube, eliminating the need for complex high temperature seals between the air and fuel streams. The air, discharged from the injector tube near the closed end of the cell, flows through the annular space formed by the cell and its coaxial injector tube. Fuel flows on the outside of the cell. Typically, 85% of the fuel is electrochemically utilized (reacted) in the active fuel cell section. The gas-impervious electrolyte does not allow nitrogen to pass from the air to the fuel side, hence the fuel is oxidized in a nitrogen free environment, averting the formation of NO<sub>x</sub>. At the open end of the cell, the remaining fuel is reacted with the air stream exiting the cell, thereby providing additional useful heat.

Because of the high generator temperature and because water vapor evolves on the anode side of the cell, reformation of natural gas and other hydrocarbon fuels can be accomplished within the generator, thus eliminating the need for an external reformer.

To construct an electric generator, individual cells are "bundled" (Figure 15) into an array of series-parallel electrically connected cells forming a mechanically stress forgiving structure that is a basic generator building block. The individual bundles are connected in series to build generator voltage and to form submodules. The parallel electrical connection of the cells within a bundle enhances generator reliability. Submodules are further combined in series to form the generator module. The generator module forms the core of Westinghouse SOFC system.

The development of a viable fuel cell electrical power generation system involves not only the development of cell and module technology, but also the development of the overall system concept, the strategy for control, and the ancillary subsystems. Field units <sup>(29,30)</sup> have served to demonstrate to customers first hand the beneficial attributes of the SOFC, to expose deficiencies through

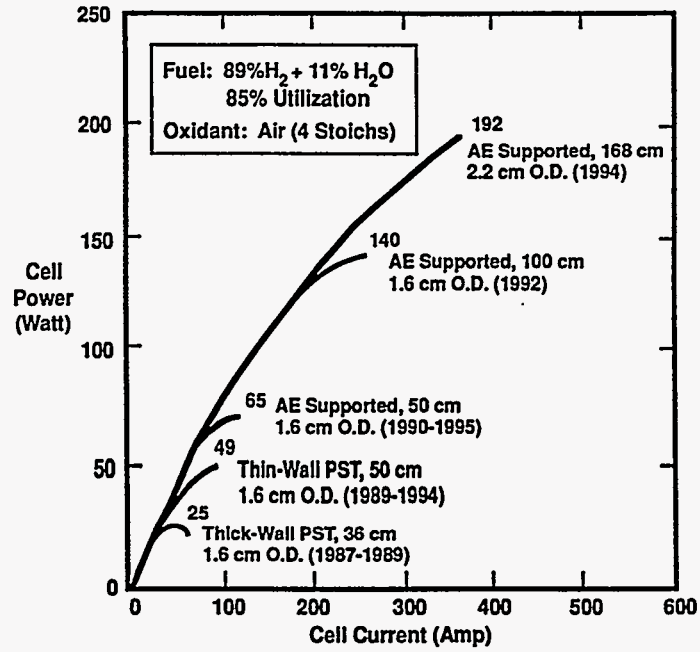


Figure 13 – Power output of different type and length solid oxide fuel cells.

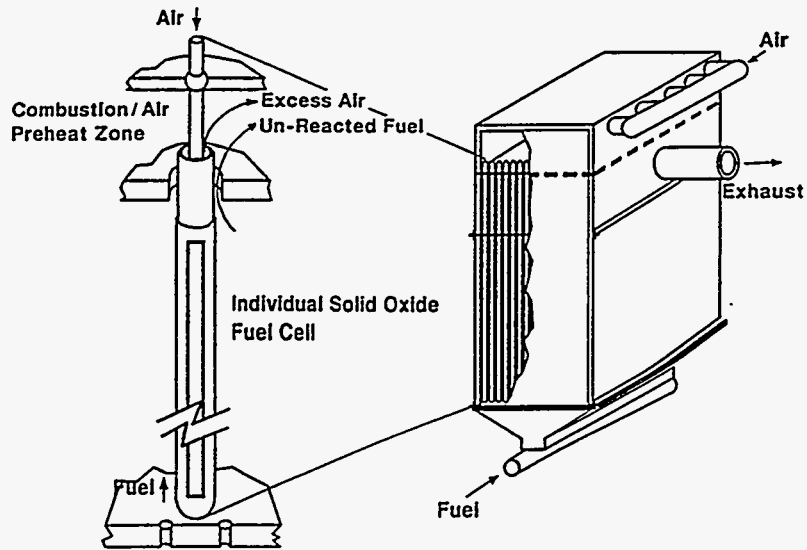


Figure 14 – SOFC seal-less module design.

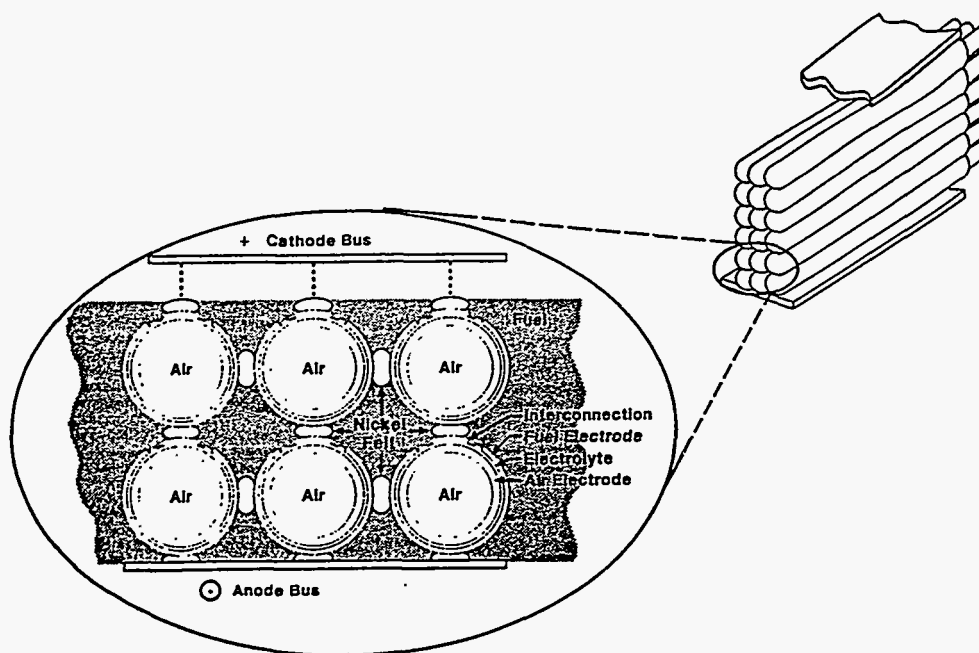


Figure 15 – Cross sections of cell bundle showing series and parallel connections.

experience in order to guide continued development, and to garner real world feedback and data concerning not only cell and stack parameters, but also transportation, installation, permitting and licensing, start-up and shutdown, system alarming, fault detection, fault response, and operator interaction.

The deployment of customer test units began in 1986 when our first experimental field unit was tested at the Tennessee Valley Authority (TVA). It was continued in 1987-88 with the two hydrogen and CO fueled 3 kW units deployed with the Osaka Gas Company, and the Tokyo Gas Company. Since 1992, Westinghouse has deployed several 20 kW class natural gas fueled SOFC generator modules (stacks) integrated into systems. The first of these was a 25 kW SOFC system deployed with The UTILITIES, a consortium of The Kansai Electric Power Company, Inc., the Tokyo Gas Company, and the Osaka Gas Company, and the second was a 25 kW cogeneration system deployed with the Joint Gas Utilities (JGU), a consortium of the Tokyo Gas Company, and the Osaka Gas Company. Most recently, a 20 kW SOFC system was deployed with the Southern California Edison Company. Table 2 provides a summary of the characteristics of Westinghouse SOFC field units to date.

Table 2  
Westinghouse SOFC Field Units

Time Year	Customer	Stack Rating (kW)	Stack Number	Cell Type	Cell Length (mm)	Cell Number	Oper. (Hrs)	Fuel	MWH
<u>Porous Support Tube Cells</u>									
1986	TVA	0.4	1	TK-PST	300	24	1760	H <sub>2</sub> +CO	0.5
1987	Osaka Gas	3	1	TK-PST	360	144	3012	H <sub>2</sub> +CO	6.1
1987	Osaka Gas	3	1	TK-PST	360	144	3683	H <sub>2</sub> +CO	7.4
1987	Tokyo Gas	3	1	TK-PST	360	144	4882	H <sub>2</sub> +CO	9.7
1992	JGU-1	20	2	TN-PST	500	576	817	PNG	10.8
1992	UTILITIES-A	20	1	TN-PST	500	576	2601	PNG	36.0
1992	UTILITIES-B1	20	1	TN-PST	500	576	1579	PNG	25.5
1993	UTILITIES-B2	20	1	TN-PST	500	576	7064	PNG	108.0
1994	SCE-1	20	1	TN-PST	500	576	5700+	PNG	91.0+
<u>Air Electrode Supported Cells</u>									
1995	JGU-2	25	1	AES	500	576	650+	PNG	
1995	SCE-2 (ARPA)	27	1	AES	500	576	TBD	PNG/DF-2/JP-8	
1996	EDB/ELSAM	100	1	AES	1500	1152	TBD	PNG	

PNG = Pipeline Natural Gas  
 TK- PST = Thick Wall Porous Support Tube  
 TN- PST = Thin Wall Porous Support Tube  
 AES = Air Electrode Supported

The generator module used in the 20 kW class SOFC customer field units is a near replica of the Multi-kW Generator (MKG) developed by Westinghouse for DOE. This module utilizes 576 cells of 500 mm active length arranged in four quadrants. Each quadrant contains eight bundles of eighteen cells. This construction is shown in Figure 16. Figure 17 shows a 20 kW SOFC generator system.

Scaleup to a multi-hundred kW and multi-MW commercial modules is the next step, and is now underway. For large applications, modules rated at several MW are planned. These modules would then be arranged in the power block concept shown in Figure 18. Any number of power blocks could then be installed to satisfy the specific requirement for large plants. Conceptual design studies have confirmed the practicality and economic feasibility of the power block concept in applications ranging up to several hundred megawatts.

#### ACKNOWLEDGMENTS

The authors acknowledge the contribution of their many colleagues whose work is reviewed in this paper. Technical work presented in this paper has been conducted under programs sponsored by the U.S. Department of Energy (DOE), the Gas Research Institute (GRI), the Westinghouse Electric Corporation and various utilities.



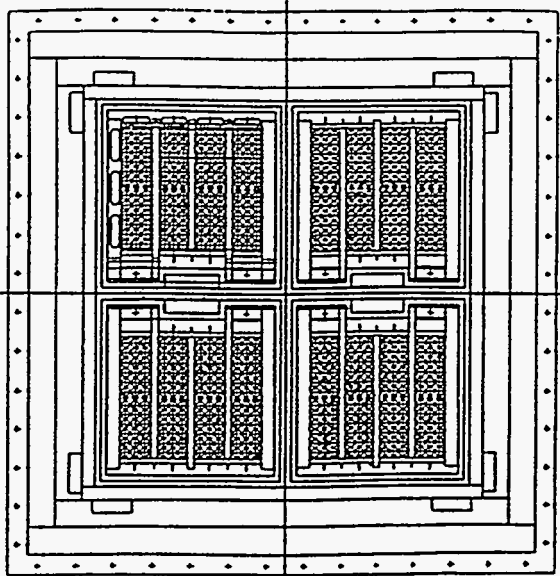


Figure 16 – SOFC generator cross section.

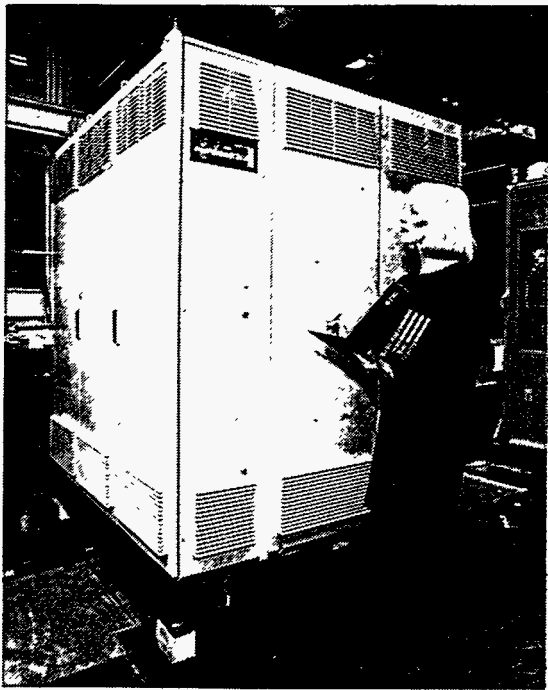


Figure 17 – 20 kW SOFC Generator System

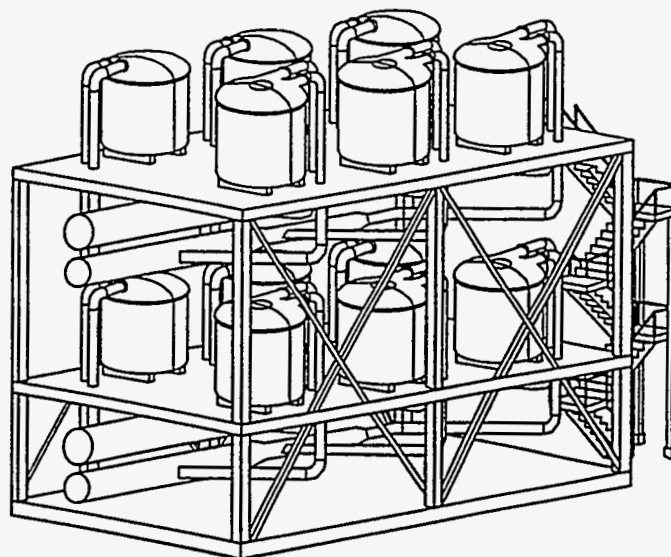


Figure 18 – SOFC power block.

#### REFERENCES

- (1) E. Baur and H. Pries, *Z. Electrochem*, 43, p. 727, 1937.
- (2) J. Weissbart and R. J. Ruka, *J. Electrochem. Soc.* 109, p. 723, 1962.
- (3) D. H. Archer, L. Elikan, and R. L. Zahardnik, *Hydrocarbon Fuel Cell Technology*, Ed. B. S. Baker, Academic Press, 1965.
- (4) R. Arcossi and E. Bergman, *J. Electrochem. Soc.* 127, p. 804, 1980.
- (5) H. S. Spacil and C. S. Tedman, *J. Electrochem. Soc.* 116, p.1618, 1969.
- (6) W. Fisher, H. Kleinsmager, F. J. Rohr, R. Steiner, and H. H. Eigsal, *Chem. Eng. Tech.*, 44, p. 726, 1972.
- (7) A. O. Isenberg, Abstracts, National Fuel Cell Seminar, Newport Beach, CA, p. 154, 1982.
- (8) A. O. Isenberg, Abstracts, National Fuel Cell Seminar, Tucson, AZ, p. 102, 1985.

- (9) N. Q. Minh, *J. Am. Ceram. Soc.*, 76, p. 563, 1993.
- (10) K. Kinoshita, F. R. McLarnon, and E. J. Cairns, *Fuel Cells A Handbook*, U.S. Department of Energy, Morgantown, WV, p. 92, 1988.
- (11) B. C. H. Steele, *High Conductivity Solid Ionic Conductors*, Ed., T. Takahashi, p. 402, 1989.
- (12) K. Z. Fung and A. K. Virkar, *J. Am. Ceram. Soc.*, 74, p. 1970, 1991.
- (13) T. Takahashi and H. Iwahara, *Energy Conversion*, 11, p. 105, 1971.
- (14) S. P. S. Badwal, *Materials Science and Technology*, Vol. 11, p. 567, 1994.
- (15) S. P. S. Badwal, *Proceedings of European Solid Oxide Forum*, Eds. Ulf Bossel, Volume 1, p. 399, 1994.
- (16) O. Toft Sorensen, *Non Stoichiometric Oxides*, Ed. O.toft Sorensen, p. 1, 1981.
- (17) A. O. Isenberg, *Proceedings of the Symposium on Electrode Materials and Processes for Energy Conversion and Storage*, the Electro Chem. Soc. Vol. 77-6, p. 572, 1977.
- (18) T. Kawada, N. Sakai, H. Yokokawa, and M. Dokia, *J. Electrochem. Soc.*, 137, p. 3042, 1990.
- (19) T. Takahashi, *Physics of Electrolytes*, Ed. J. Hladik, p. 989, 1972.
- (20) O. Yamamoto, Y. Takeda, R. Kanno and M. Noda, *Solid State Ionics*, 22, p. 241, 1987.
- (21) H. Yokokawa, N. Sakai, T. Kawada and M. Dokia, *Denki Kagaku*, 58, p. 489, 1990.
- (22) R. J. Ruka, *Workshop on High Temperature Fuel Cells*, Brookhaven National Laboratory, Upton, NY 1977.
- (23) R. J. Ruka and P. Singh, *3rd Workshop on Purification of Metals for Crystal Growth and Glass Processing*, Orlando, FL, 1989.

- (24) Ceramatec Inc., Report No. GRI-87/0297, Gas Research Institute, Chicago, IL, 1989.
- (25) S. Nagata, Y. Ohno, Y. Kasuga, Y. Kaga, and H. Sato, Proceedings of the 19th IECEC, American Nuclear Society, p. 827, 1984.
- (26) D. C. Fee et al., National Fuel Cell Seminar, Tucson, p. 40, 1986.
- (27) P. Singh, R. J. Ruka, and R. A. George, Proceedings of the 24th IECEC, Institute of Electronics and Electrical Engineers, p. 1553, 1989.
- (28) P. Singh, R. J. Ruka, and R. A. George, U.S. Patent 4894297, 1990.
- (29) S. E. Veyo, A. Kusunoki, S. Kaneko, and H. Yokoyama, A Solid Oxide Fuel Cell Power System in 1992/1993 Field Operation, in Proceedings of American Power Conference, Vol. 56-1, pp. 159-165, 1994.
- (30) R. J. Bratton, "Westinghouse Solid Oxide Fuel Cell Developments", in Proceedings of First European Solid Oxide Fuel Cell Forum, October 1994.